Accepted manuscript

Norwegian Journal of Geology

Quantification of time-varying groundwater flow in boreholes in fractured crystalline rock using long-term distributed temperature sensing

Karoline Husevåg Kvalsvik, Randi Kalskin Ramstad, Henrik Holmberg & Kirsti Midttømme

DOI: https://dx.doi.org/10.17850/njg102-1-1

Article number: 202201

Received 08. July 2021 / Accepted 04. January 2022 / Published online xx.xx.xx

Refer to this publication as:

Kvalsvik, K. H., Ramstad, R. K., Holmberg, H. & Midttømme, K., 2022: Quantification of time-varying groundwater flow in boreholes in fractured crystalline rock using long-term distributed temperature sensing. Norwegian Journal of Geology 101, 202117. https://dx.doi.org/10.17850/njg102-1-1

Quantification of time-varying groundwater flow in boreholes in fractured crystalline rock using long-term distributed temperature sensing

Karoline Husevåg Kvalsvik[1,2], Randi Kalskin Ramstad[1,3], Henrik Holmberg[3] & Kirsti Midttømme[2]

[1] Norwegian University of Science and Technology (NTNU), S. P. Andersens veg 15a, 7031 Trondheim, NORWAY

[2] Norce Norwegian Research Centre AS, Postboks 22 Nygårdstangen, 5838 Bergen, NORWAY

[3] Asplan Viak AS, Hotellgata 2, 7500 Stjørdal, NORWAY

E-mail corresponding author (Karoline Husevåg Kvalsvik): karoline.kvalsvik@ntnu.no

Quantification of groundwater flow is an important factor for several applications, such as water supply, boreholes for energy extraction/storage and drainage and flood prevention projects. In this study, distributed temperature sensing (DTS) with fibre-optics has been combined with energy calculations to estimate the time-varying groundwater flow in fractures in four stand-alone boreholes at Åkneset in Norway. The method captures the natural, undisturbed time-variation of the groundwater flow as no tracers or pumps were used. Compared with temperature profile measurements using a probe, long-term distributed temperature sensing (from several weeks) gives a profound understanding of the hydrogeological conditions for a site. One example of how long-time measurements enhance this understanding is that they provide information about the sources of the groundwater flow: For some fractures, the groundwater estimations showed no correlation with meteorological data, indicating that these fractures are fed from deeper regional flow, with relatively large response times. In other fractures, the temporal variations in estimated groundwater flow showed high correlation (>0.60) with precipitation or temperature, with 1.4–9.0 days delay. This indicates that these fractures are fed mainly from precipitation and snow melting. The correlation with weather conditions at the surface also indicates that the method gives a true time-variation of groundwater flow. The results

from the study show that DTS can be a useful tool to quantify groundwater flow in boreholes made for energy and monitoring (e.g., in tunnels). The method could be further improved by injection of heat along the entire borehole length, which has been done before. This would be similar to a thermal response test, which is an important pre-investigation for borehole thermal energy storage.

Keywords: Groundwater flow, Groundwater quantification, Distributed Temperature Sensing (DTS), Åkneset, Borehole monitoring,

Introduction

Borehole thermal energy storage (BTES) can significantly enhance the share of renewable energy as it allows storage of renewable/waste heat or cold for later use (Mesquita et al., 2017; Energiforsk, 2019). Thermal energy storage can be achieved by drilling several boreholes into the ground to inject and extract heat through these holes to and from the ground (Mesquita et al., 2017). In Finland, Sweden and Norway, the bedrock is typically crystalline rock. Permeable fractures are the main flow path for groundwater, which enables groundwater flow if a hydraulic gradient is present. Fractures enable better heat transfer contact with the ground, which is desirable. On the other hand, regional groundwater flow through a BTES would cause a heat loss (Gehlin & Hellström, 2003). Thus, it is desirable to quantify the natural/undisturbed/regional groundwater flow to evaluate if the loss is acceptable; if present, fractures should be filled to reduce the loss as demonstrated in (Energiforsk, 2020), or if the site is unsuited for storage.

Current pre-investigation methods for BTES sites include a thermal response test (TRT). TRT is a field test to determine properties of the ground, such as the effective thermal conductivity of the ground. A TRT can reveal groundwater flow (Liebel et al., 2011), but not how much and which parts of the borehole that are affected. This is not the goal with the test. Heat injection also induces the thermosyphon effect: vertical groundwater flow due to density changes in the heated water, so that the groundwater flow is affected by the test.

Several studies have estimated borehole yield or velocity of groundwater by means of, among other techniques: chemical tracer (Guihéneuf et al., 2017); thermal tracer (Leaf et al., 2012; Read et al., 2013; Banks et al., 2014; Acuña et al., 2018); pumping tests (Ramstad, 2004; Banks et al., 2014); modelling and parameter fitting (Klepikova et al., 2011; Li et al., 2020) and energy balance (Read et al., 2013).

A common feature of these studies are that they consider momentary values for groundwater flow and/or injected water into the fractures so that the natural groundwater flow was disturbed. Hence, none of them investigates the time-variation of the natural groundwater flow. Some of the studies (Ramstad, 2004; Read et al., 2013; Guihéneuf et al., 2017) utilised the fact that two or more boreholes are intersected by the same fracture(s), and used pumping in one/more boreholes to enhance flow through the connecting fracture(s). Use of a thermal tracer in stand-alone boreholes is a way to measure vertical groundwater flow in the borehole (Leaf et al., 2012; Banks et al., 2014; Acuña et al., 2018). Hence, if groundwater enters and leaves the borehole at the same depth, it cannot be quantified by this method.

Read et al. (2013) injected hot water and pumped out cold water from the borehole to estimate the groundwater flow through the fracture. This article develops and demonstrates a method to quantify the undisturbed, time-varying groundwater flow entering stand-alone boreholes through fractures, regardless of whether or not the groundwater flow contributes to the vertical groundwater flow in the borehole. This is not measurement of the groundwater level, but an estimation of the horizontal groundwater flow in fractures. Groundwater quantification is done by applying an energy balance similar to that of Read et al. (2013) but adding the temporal change and conductive terms to see if there is time variation in the groundwater flow and if conduction is truly negligible. Another important difference from the work of Read et al. (2013) is that the proposed method avoids both pumping and thermal injection as this may disturb the natural groundwater flow. The resulting groundwater flowrates are thereafter compared to temperature and precipitation data to reveal details of how the water has travelled from the surface to the fractures. Various response times for the estimated groundwater flow compared to climate data were tested, and the response times giving the highest correlation factors are reported together with the highest correlation factors achieved.

Method

The groundwater flow in a fracture may be determined from energy balance and temperature measurements (Read et al., 2013). Here, this method is extended to include the transient term (see equation 1) and applied to temperature profiles from four boreholes, made available for this study and measured at Åkneset, Norway.

Åkneset - site description

Åkneset is a mountain side underlain mostly of mica-rich gneiss (Kveldsvik, 2008) that moves/slides towards the underlying fjord in western Norway, see Fig. 1. The information about the site provided in this section is from NVE (2021) unless otherwise stated. The mountain edge behind Åkneset is about 1100–1400 metres above mean sea level (amsl). From about 700–1000 amsl, there is a backscarp below which the mountain side moves 2–8 cm south-southwest each year. When it eventually slides down into the fjord below, 18–54 million m^3 of rock will cause a tsunami which will hit several communities in the surrounding fjords. A worst-case scenario will generate a wave about 80 m high (Linge, 2021; NVE, 2021).

Several studies on stability at Åkneset have been performed (Kveldsvik, 2008; Grøneng, 2010). Water runs through a network of fractures in the mountain (Kveldsvik, 2008). Modelling has shown that draining can stabilise the mountain side (Kveldsvik, 2008). The site is monitored through several boreholes to estimate movement and eventually drain the mountain side to prevent or reduce the impact of a landslide (Kveldsvik, 2008; NVE, 2021). The placements of the boreholes at Åkneset are shown in Fig. 1. This study treats data from the boreholes KH-01-17 and KH-02-17, drilled in 2017, and KH-01-18 and KH-02-18, drilled in 2018. Data for the boreholes are given in Table 1.

Distributed temperature sensing using fibre-optics

Temperature measurements were carried out by Acuña et al., (2018) using fibre-optic distributed temperature sensing where a glass fibre is lowered into the borehole. Light pulses are sent through the fibre and backscattered light is measured. Temperature can then be determined from built-in parameters in the measurement equipment, a XT-DTS Silixa. More details of the measurement technique can be found in Hausner et al. (2011), van de Giesen et al. (2012) and McDaniel et al. (2016). The measurement setup is illustrated in Fig. 2 of Acuña et al.(2018) and involves coupling the measurement equipment to one end of one or more fibre cable(s). The other ends of the fibre cables were lowered into the boreholes. Between the borehole(s) and the measurement equipment, the fibre cables were coiled up and the coils placed in a calibration bath. Calibration consisted of measuring the temperature of the calibration bath by an external temperature probe. This external temperature measurement was used to adjust the temperature to the correct level. Temperature measurements presented here are for every 0.25 m and 100 min (2018-boreholes) or 150 min (2017-boreholes).

Groundwater estimation

Horizontal groundwater flow intersecting a borehole with a different temperature than the borehole will create deviations in the temperature profile (Drury et al., 1984; Liebel et al., 2011). Defining a control volume around these deviations, an energy balance for this control volume may be made from which the groundwater flow in the fractures can be estimated. Defining the variables described in Fig. 2, the energy balance is:

$$\dot{m}_{in}(T_{in} - T_{ave})c_p + \dot{Q}_{top} + \dot{Q}_{bottom} + \dot{m}_{vertical,top}(T_{top} - T_{ave})c_p = m_V c_p \frac{\partial T_{ave}}{\partial t} \qquad 1$$

where $\dot{m}_{in}$[kg/s] is a mass flow of water at temperature T_{in} [°C], entering the volume through a fracture, and leaving the volume at temperature T_{ave} [°C]; $\dot{m}_{vertical,top}$ [kg/s] is the vertical, downwards mass flow of water in the borehole, entering at temperature T_{top} [°C] and leaving at temperature T_{ave} [°C]; c_p [J/kg/°C] is the specific heat capacity of water; m_V is the mass of the water in the volume; $\frac{\partial T_{ave}}{\partial t}$ [°C/s] is the rate of change in average temperature in the volume with time t [s]; $\dot{Q}_{top}$and $\dot{Q}_{bottom}$ [W] are conductive heat into the volume from the top and bottom of the volume, respectively. These are related to the thermal gradient in the rock.

For a given control volume, the mass m_V is found from multiplying the volume by the water density. The temperature above the volume (T_{top}) and the average temperature in the volume (T_{ave}) are known from the DTS-data as functions of time.

To determine the other terms in equation 1 and estimate the groundwater flow in the fractures, the following assumptions were made:

- Physical properties of the groundwater are known, constant values: specific heat capacity is 4210 J/kg/K, thermal conductivity is 0.576 W/K/m and water density is 1000 kg/m^3.
- The boreholes are in steady-state and in thermal equilibrium with the surrounding rock.
- Internal heat production due to radiogenic decay is negligible (Slagstad et al., 2008).

- Thermal radiation is negligible.
- Vertical groundwater flow in the boreholes ($\dot{m}_{vertical,top}$) is constant and equal to the product of the water density, the boreholes' cross-sectional area and the median velocities found by Acuña et al. (2018, 2020). Fig. 3 shows a summary of their results. The used values are presented in Table 2.
- The term $m_V c_p \frac{\partial T_{ave}}{\partial t}$ in equation 1, i.e., the change in energy in the volume, can be estimated from measured DTS data by

$$\frac{\partial T_{ave}}{\partial t} \approx \frac{T_{ave,i} - T_{ave,i-1}}{\Delta t} \tag{2}$$

where i is the index of temporal measurement and Δt the time increment.

- Vertical conduction in the borehole, $\dot{Q}_{top}$ and $\dot{Q}_{bottom}$, follow Fourier's law:

$$\dot{Q}_{top/bottom} = \pm A\lambda \frac{\partial T}{\partial z} \tag{3}$$

where λ is the thermal conductivity of water, A is the area the groundwater flows through, T is temperature and z is depth. Hence, $\dot{Q}_{top}$ and $\dot{Q}_{bottom}$ can be estimated from the known borehole dimensions, water thermal conductivity and the measured DTS data by

$$\frac{\partial T}{\partial z} \approx \frac{T_{i+3} - T_{i-3}}{6 * \Delta z} \tag{4}$$

where i is index of the temperature measurement at the border of the control volume and Δz is the distance between two temperature measurements. Using i ± 3 as a compromise between using values remote from the border to neglect the influence of measurement noise and using local values to be more precise.

- The temperature of the outflowing groundwater is equal to the average temperature T_{ave} in the control volume: due to this, terms related to outflowing groundwater ($\dot{m}_{out}$ *and* $\dot{m}_{bottom}$) are not present in equation 1 as the temperature differences become zero, see Fig. 2.
- For control volumes with *lower* temperature than the surroundings, the inlet temperature of the horizontal groundwater flow equals the *lowest measured temperature* in the volume during the

measurement period. This was done because the groundwater flow in the fracture zone is considered the cause of the locally lower temperature, and the groundwater flow can only cause the lowest measured temperature in the volume, by having a temperature at least as low. Similarly, for control volumes with *higher* temperature than its surroundings, the *highest* measured temperature was used as inlet temperature from the fracture zone.

Using these assumptions, the only energy flows into and out of the control volume are those following vertical and horizontal groundwater flow and vertical conduction, see Fig 2; and the only unknown in equation 1 is $\dot{m}_{in}$, the mass flow of groundwater in through the fracture. Solving for $\dot{m}_{in}$, an equation to estimate the groundwater flow in fractures using the DTS data results:

$$\dot{m}_{in} = \frac{m_V c_p \frac{\partial T}{\partial t} - Q_{top} - Q_{bottom} - \dot{m}_{vertical,top}(T_{top} - T_{ave}) c_p}{(T_{in} - T_{ave}) c_p} \qquad 5$$

Equation 5 will give one value per time step. As the temperatures of the horizontal groundwater flows are estimates, calculated groundwater flows will also be estimates. Since the lowest/highest temperature is used as the inlet temperature, the resulting groundwater flow gives the largest value of $(T_{in} - T_{ave})c_p$ and thus the lowest value of $\dot{m}_{in}$ one can justify in the calculation. Results were compared to the increase in groundwater flow velocities in other studies (Acuña et al., 2018, 2020).

The lowest temperatures in the boreholes from 2017 were all adjacent to a period without measurement data (2nd–4th of July 2018) and markedly lower than all other measured temperatures in the volumes, suggesting that they are erroneous. Therefore, both the lowest and the second lowest measured temperature were used as inlet temperature. The second lowest measured temperature used in the calculations was not affected by the period of missing data.

Uncertainty estimation

To estimate the uncertainty of the method, it was also applied to some sections without visible flow, for which expected values and standard deviations from measurement noise are reported.

Correlation with precipitation

Precipitation and ambient temperature data from Åknes weather station (c. 900 amsl, see Fig. 1) were provided by the Åknes project. The estimated groundwater flows in the boreholes at Åkneset were compared to meteorological data by means of a correlation coefficient. A correlation would reveal if the groundwater flow is connected to some surface phenomenon and, if so, where the origin of the groundwater flow may be (Sena & Braathen, 2020). The correlation coefficient for two datasets X and Y with n datapoints x_i and y_i, and mean values $\hat{x}$ and $\hat{y}$, this is defined as (Walpole et al., 2007):

$$Corr(X,Y) = \frac{\sum_{i=1}^{n}(x_i - \hat{x})(y_i - \hat{y})}{\sqrt{\sum_{i=1}^{n}(y_i - \hat{y})^2 \sum_{i=1}^{n}(x_i - \hat{x})^2}} \qquad 6$$

The correlation coefficient is 0 for non-correlated data, + 1 for perfectly correlated data and - 1 for perfectly, but opposite correlated data (positive change in one dataset moves up for every negative change in the other and vice versa). Moving daily averages of mass groundwater flow and precipitation were used in equation 6 to exclude the effect of measurement noise. The datasets were also adjusted in time relatively to each other because there is expected to be a delay between meteorological data and correlated groundwater flow.

Measurement data

Measured temperatures in the boreholes as a function of time are shown in Fig. 4. The temperature profiles shifted up and down by about 0.5°C during the measurement periods, suggesting that the water columns were heated and cooled. As the change is consistent over the whole temperature profile (except in KH-01-18) and clearly larger than the measurement noise, this is considered to be a true temperature variation. This may be caused by the vertical flow, even if very small, along the entire depth of the boreholes. Thus, less flow is expected in the part of KH-01-18 where the profile shifts are significantly smaller, see Fig. 4. The profiles in KH-01-17 and KH-02-17 do not shift up and down at the same time, suggesting that they are fed from different sources.

Identified depths for potential fractures are marked by grey stippled lines in Fig. 4. Fractures were detected by inspecting the temperature profiles and noting where irregularities/changes in the profiles occurred consistently for all times.

KH-01-17

Some irregularities in the temperature profiles (Fig. 4) for this borehole are seen between 75 and 100 m depth, which are larger than the measurement noise and apparent during the entire measurement period. Hence, these are probably caused by groundwater flow in fractures and were thus investigated in this study using equation 5. The irregularities between 100 and 150 m in the temperature profile in KH-01-17 on 13th June are present for too short a period for flow evaluation.

KH-02-17

The groundwater flow in KH-02-17 apparently vanishes at about 275 m depth (Acuña et al., 2018). This is clearly seen by the change in slope and temperature at this depth. The measurement noise appears to increase strongly below 200 m in KH-02-17. A possible explanation for the increased noise is that the flow moves the fibre cable used for measurements, causing stresses in the fibre cable and variation in temperature measurements.

KH-01-18

Borehole KH-01-18 shows high time variation and irregularity in the temperature profile above c. 130 m. The temperature peaks in the profile are many and vary with time. It was decided to choose one of the highest peaks which was visible in nearly all profiles. This peak is located at about 75 m depth. As the slope of the entire profile changes at about 133 and 198 m, these depths were also considered.

KH-02-18

In borehole KH-02-18 there are several temperature peaks on the first measurement day, but their duration is so short that it was assumed to be unlikely to obtain results for these peaks. To see if this assumption holds, one peak (at 138 m) was included in the analysis, together with potential fractures at 90 and 125 m where changes in measurement noise and slope were found.

Results

The estimated groundwater flow in fractures in KH-02-18 resulting from equation 5 is shown in Fig. 5. As the measurement noise hides trends in the results, only moving averages are shown for the other fractures and boreholes. These are shown together with their correlation with climate data in Figs. 6, 7, 8 & 9.

Highest correlation factors were found for 3.8, 3.9 and 3.9 days for the fractures in KH-01-17 in increasing order. For KH-02-17, no higher correlation with precipitation than 0.17 was found, and for KH-01-18, no higher correlation factor than 0.11 was found. The fracture at 75 m gave a correlation factor of 0.68 with ambient temperature when the temperature data were moved 9.0 days ahead in time, see Fig. 9. No flow was found at 90 or 138 m depth in KH-02-18. The groundwater flow at 125 m depth in KH-02-18 showed no clear correlation with precipitation, but a correlation factor of 0.84 with temperature was found for a time delay of 1.4 days; see Fig. 9.

Applying the same method to some sections without visible fractures, the expected flow values are all close to 0 and negative (see Table 3) as the advective term dominates in equation 5. For KH-02-17, the standard deviations are lower than in KH-01-17, and the uncertainty (1.96 standard deviations) is less than about 1 l/h.

Inspecting the value of each term in equation 5 (not shown), it was found that the conductive heat was negligible compared to the advective terms (about 10^5 times smaller).

Discussion

The proposed method gives a rough estimate for minimum groundwater flow which seems to vary with time, especially in KH-01-17, KH-02-18 and the upper part of KH-01-18. Several of the obtained values correlate with climate data, indicating that the estimates are truly related to the groundwater flow in the fractures, as they are connected to surface weather conditions. The groundwater level in Åkneset has previously been found to depend on meteorological data (Sena & Braathen, 2020).

Estimated groundwater flow in KH-01-17 is lower than the uncertainty in this borehole (standard deviation is about 2.6 l/h from Table 3, giving an uncertainty of 5.1 l/h). However, the expected value is negative, and the fractures considered in KH-01-17 are visible in all temperature profiles. Thus, the estimates in KH-01-17 are believed to be >0, but their exact values are not found.

In KH-02-17, the estimated groundwater flow is typically at least one order of magnitude higher than the uncertainty in KH-02-17. The measurement noise in the boreholes from 2018 is similar to that in KH-02-17 below 200 m depth and the vertical groundwater velocity is lower. From equation 5, the uncertainty increases with vertical velocity. Hence, the uncertainty in these two boreholes is expected to be no larger than in KH-02-17, and no uncertainty estimation was performed for these boreholes.

Based on the calculated uncertainties, groundwater flow estimations in KH-02-17, KH-01-18 and KH-02-18 are probably close to their true values, with uncertainties of about 1 l/h, whereas the flow in KH-01-17 is probably somewhere between 0 and about 5.5 l/h (A 95% confidence interval is: expected value ± 1.96 std deviations (Walpole et al., 2007). Expected values are ≈ 0.3 l/h and standard deviations are ≈ 2.6 l/h in Table 3, yet the values should be nonzero, giving 0–5.5 l/h.)

In borehole KH-01-17, all the groundwater flow estimates showed high correlation factors of 0.60–0.69 with precipitation. In borehole KH-02-17, no correlation with precipitation is found. This differs from previous findings, where a correlation between the groundwater level in KH-02-17, and potentially also the hydraulic head at 101 m, precipitation and snow melt was detected (Sena & Braathen, 2020). However, the summer 2018 was unusually warm and dry. It is possible that all snow had already melted when the measurements in KH-02-17 were performed, so that this correlation could not be detected. Large groundwater flow was found here for KH-02-17 despite the dry summer. This corroborates the findings of Sena & Braathen (2020), who also assumed that these streams stem from a larger reservoir. The measurements in the boreholes from 2018 were performed during summer 2019. Unlike KH-02-17, the groundwater flow in KH-02-18 shows a clear dependence on temperature/snow melt.

The estimated groundwater flow in KH-02-17 and the lower part of KH-01-18 is two orders of magnitude higher than in borehole KH-01-17 and the fracture at 75 m depth in KH-01-18. This suggests that the fractures in borehole KH-02-17 and the lower part of KH-01-18 are fed from a lake. The fractures in borehole KH-01-17 and upper KH-01-18 are directly from precipitation or reservoirs which depend on precipitation. Only a lake or other large water reservoir would be able to supply a large and stable groundwater flow as observed in KH-02-17 and KH-01-18, apparently unaffected by precipitation. One of the most likely water reservoir sources is Instevatnet ("the Innest lake"). However, Sena & Braathen (2020) found that Instevatnet or other lakes behind the mountain edge probably have very limited effect. Still, the deepest fractures in this study are >100 m deeper than the fractures considered in their study. Thus, Instevatnet may still be the source for the deepest fractures.

The groundwater flow in KH-01-17, the upper part of KH-01-18 and at 125 m depth in KH-02-18 are unlikely to stem from a large water reservoir just because they reflect the climate data. Groundwater may flow through different paths/fractures before entering the boreholes (Sena & Braathen, 2020), and thus may consist of several contributions with different time delays. This could explain why the correlation was not even higher. If some of the groundwater flow in KH-01-17 stems from surface water in soil/vegetation, parts of it would evaporate instead of entering the fractures. This would explain why some precipitation peaks do not show any corresponding peaks in the groundwater flow estimations.

The estimated groundwater flow is more evenly distributed than the precipitation data. Hence, some degree of storage (in vegetation, soil or ponds) is probably present for the weather-dependent groundwater flow, but to a smaller extent than for KH-02-17, KH-02-18 and the lower part of KH-01-18. These findings are in line with the fact that KH-01-17 lies in the area where groundwater flow stems mainly from “Direct infiltration from rain and snow melt” (Sena & Braathen, 2020). The other three boreholes are placed in the fastest moving parts of Åkneset (Sena & Braathen, 2020; NVE, 2021). This part of the mountain side is fed from groundwater flow in the backscarp (Sena & Braathen, 2020), and lies above the streams which showed high, stable flow all summer, even during 2018 (Sena & Braathen, 2020). Thus, a larger, more stable groundwater flow is expected in these boreholes than in KH-01-17. The groundwater flow in borehole KH-02-17 shows an abrupt step at the period without data. No explanation for this has been found.

The positions of the active fractures in KH-01-17 and KH-02-17 found in this work correspond to the findings of Acuña et al. (2018) and Elvebakk & Pless (2018). A comparison of where active fractures are found in previous studies vs. this study is given in Table 4. The positions of active fractures in the boreholes from 2018 do not show good agreement with previous studies. Elvebakk & Pless (2018) reported other active fractures in these boreholes than those found here. However, they also reported a different flow pattern and groundwater level than observed by Acuña et al. (2020). As to when the boreholes were relatively new, a possible explanation is that the new boreholes form new pathways for water, which could have led to large initial flows from some reservoirs which may later have been emptied. A lower, semi-steady-state flow could then have been established when the investigations of Acuña et al. (2020) were performed. As the measurements in this study stem from either directly before or after the measurements of Acuña et al. (2018, 2020), their flow pattern is believed to be most correct for this work. However, it is clear that the groundwater flows at Åkneset are not constant.

Most of the changes in vertical groundwater flow reported by Acuña et al. (2018, 2020) at depth are either constant or decreasing when passing the fractures considered in this study. This work estimates groundwater flow *into* the boreholes, and thus, the values cannot be compared in most cases. Two exceptions are the fracture at about 123 m depth in KH-02-17, where the vertical groundwater flow increases from about 0.47 to about 0.67 m/min (Acuña et al., 2018) and the fracture at 125–130 m depth in KH-02-18, where the vertical velocity of about 0.16 m/min starts (Acuña et al., 2020). With the borehole radius of 48 mm and water density of about 1000 kg/m^3, a net change of 0.67–0.47 min/m means that about 43 or 87 l/h enters the borehole at 123 m depth in KH-02-17, depending on whether the velocity is assumed to be the average or maximum velocity (laminar regime). This study assumes that velocities in Acuña et al. (2018) are average velocities, corresponding to the value of 87 l/h, which is about twice as much as estimated in Fig. 7. However, the results are of the same magnitude. Using the same method for the inflow in KH-02-18, the flow should be about 35 or 69 l/h. Fig. 9 (right) shows a typical groundwater flow of about 20 l/h, with peaks up to about 45 l/h. Thus, results are again of the same order of magnitude. Since this study provides a *minimum* estimate for the groundwater flow, and the groundwater flow varies with time, these two results may be said to show agreement between the two studies.

The estimations of groundwater flow in Elvebakk & Pless (2018) are about one order of magnitude larger than the values found here. This supports the hypothesis that the boreholes had a high initial groundwater flow when they were new, which later have drained some of the reservoirs so that the groundwater flow now has reached a lower semi-steady state. However, the results in this work cannot be said to agree with those of Elvebakk & Pless (2018).

Better groundwater flow estimations could have been achieved if heat was injected along the entire borehole length, as this would reveal all fractures with groundwater flow. It would also improve the accuracy and precision of the estimated groundwater flow as the upper possible limit for the groundwater flow would no longer be infinite (T_{in} - T_{ave} in equation 5 would not be 0 if the borehole temperature T_{ave} is raised) and the relative error in guessing the inlet temperature would be smaller the higher the difference between guessed T_{in} and T_{ave}.

Conclusions

The use of DTS and energy balance provides an estimate for the time-dependent minimum groundwater flow in fractures when the vertical groundwater flow is known. The results show that the groundwater flow in several fractures varies with time at Åkneset. Thus, direct comparison of results between studies is difficult, but the obtained groundwater flow estimates are of the same order of magnitude as in previous investigations performed directly before or after the measurements considered here. Here, the estimations are generally lower (about 50%), but they are *minimum* estimates. Compared to groundwater flow estimates from the time when the boreholes were new, the results are an order of magnitude lower. One possible explanation is that new boreholes form new pathways for groundwater, with high initial groundwater flow while draining some water reservoirs before reaching a semi-steady state with a lower groundwater flow.

The groundwater flow rates in borehole KH-01-17 are low (≈ 0.0–2.0 l/h) and correlated with precipitation (correlation factors of 0.60–0.69) with about 4 days delay, suggesting that these fractures are fed from direct infiltration of surface water, perhaps with some intermediate storage in vegetation. Estimated groundwater flows in KH-02-17, KH-01-18 and KH-02-18 show no clear correlation with precipitation. All three have large groundwater flows of tens of litres per hour. The groundwater flow in KH-02-18 is clearly correlated with snow melt (correlation factor of 0.84). The groundwater flow in the upper part of KH-01-18 also showed some correlation with snow melt (correlation factor of 0.68), whereas groundwater flow in KH-02-17 and the lower parts of KH-01-18 is not clearly correlated with climatic data. These stable, high groundwater flow rates, independent of climatic data, indicate that the fractures are fed from one or more larger reservoirs, which has also been suggested in previous studies.

The results and method are relevant for boreholes for extraction, injection and/or storage of thermal energy and draining projects like the one at Åkneset. The proposed method for estimation of groundwater flow would be even more informative if heat was injected along the entire borehole length, so that there would be a larger difference between the temperature of the groundwater flowing water and the water in the borehole.

Acknowledgements. The authors wish to express their deepest thanks to NVE and their project on enhancing knowledge about draining of Åknes for supplying data for this study. Thanks also go to the Norwegian Research Council and the partners of the RockStore project (grant no. 281000) for the funding of this work. In addition, thanks go to the reviewers James Tinjum and Victor Bense for their help to improve the manuscript quality.

References

Acuña, J., Malmberg, M., Acuña, F. & Stokuca, M. 2018: ÅKNES - Heat Tracing Tester, KH-01-17 och KH-02-17, Stockholm. *Bengt Dahlgren AB Report nr. 22301-1.1*, 34 pp.

Acuña, J., Ramstad, R. & Pless, G. 2020: Vertical groundwater movement identification through Distributed Heat Tracing Tests. Case of Åknes, Norway. *14th Congress INTERPRAEVENT, 31 May–2 June 2021, virtual congress.*

Banks, E.W., Shanafield, M.A. & Cook, P.G. 2014: Induced temperature gradients to examine groundwater flowpaths in open boreholes. *Groundwater 52*, 943–951. https://doi.org/10.1111/gwat.12157.

Drury, M.J., Jessop, A.M. & Lewis, T.J. 1984: The detection of groundwater flow by precise temperature measurements in boreholes. *Geothermics 13*, 163–174. https://doi.org/10.1016/0375-6505(84)90013-0.

Elvebakk, H. & Pless, G. 2018: Borehullslogging Åknes, Stranda kommune 2017-2018. *NGU Report 2018.026*, 70 pp.

Energiforsk. 2019: Värdet av säsongslager i regionala energisystem. *Energiforsk Report 2019:624*, 64 pp.

Energiforsk, 2020: Impermeable boreholes for high temperature thermal energy storage. *Energiforsk Report 2020:666*, 67 pp.

Gehlin, S. & Hellström, G. 2003: Influence on thermal response test by groundwater flow in vertical fractures in hard rock. *Renewable energy 28*, 2221–2238. https://doi.org/10.1016/S0960-1481(03)00128-9.

Grøneng, G. 2010: *Stability Analyses of the Åknes Rock Slope*, *Western Norway*. PhD thesis, Norwegian University of Science and Technology, 169 pp.

Guihéneuf, N., Bour, O., Boisson, A., Le Borgne, T., Becker, M.W., Nigon, B., Wajiduddin M., Ahmed, S. & Maréchal, J.-C. 2017: Insights about transport mechanisms and fracture groundwater flow channeling from multi-scale observations of tracer dispersion in shallow fractured crystalline rock. *Journal of Contaminant Hydrology 206*, 18–33. https://doi.org/10.1016/j.jconhyd.2017.09.003.

Hausner, M.B., Suárez, F., Glander, K.E., van de Giesen, N., Selker, J.S. & Tyler, S.W. 2011: Calibrating single-ended fiber-optic Raman spectra distributed temperature sensing data. *Sensors 11*, 10859–10879. https://doi.org/10.3390/s111110859.

Kartverket. 2021: Norgeskart https://norgeskart.no/#!?project=norgeskart&layers=1002&zoom=3&lat=7197864.00&lon=396722.00 (accessed 2. February 2021).

Klepikova M.V., Le Borgne, T., Bour, O. & Davy, P. 2011: A methodology for using temperature-depth profiles under ambient, single and cross-borehole pumping conditions to estimate fracture hydraulic properties. *Journal of Hydrology 407*, 145–152. https://doi.org/10.1016/j.jhydrol.2011.07.018.

Kveldsvik, V. 2008: *Static and dynamic stability analyses of the 800m high Åknes rock slope, western Norway*. PhD thesis, Norwegian University of Science and Technology, 105 pp. https://doi.org/10.1016/j.ijrmms.2008.10.007.

Leaf, A.T., Hart, D.J. & Bahr, J.M. 2012: Active thermal tracer tests for improved hydrostratigraphic characterization. *Groundwater 50*, 726–735. https://doi.org/10.1111/j.1745-6584.2012.00913.x.

Li, B., Han, Z., Hu, H. & Bai, C. 2020: Study on the effect of groundwater flow on the identification of thermal properties of soils. *Renewable Energy 147*, 2688–2695. https://doi.org/10.1016/j.renene.2018.06.108.

Liebel, H.T., Huber, K., Frengstad, B.S., Ramstad, R.K & Brattli, B. 2011: Temperature footprint of a thermal response test can help to reveal thermogeological information. *NGU Bulletin 451*, 20–31.

Linge, H. 2021: *Åkerneset*. https://snl.no/%C3%85kerneset (accessed 27. January 2022).

McDaniel, A., Harper, M., Fratta, D., Tinjum, J., Choi, C. & Hart, D. 2016: Dynamic Calibration of a Fiber-Optic Distributed Temperature Sensing Network at a District-Scale Geothermal Exchange Borefield. *In* Farid, A., De, A., Reddy, K.R., Yesiller, N. & Zekkos, D. (eds.): *Geo-Chicago 2016: Geotechnics for Sustainable Energy*, American Society of Civil Engineers, pp. 1–11. https://doi.org/10.1061/9780784480137.001.

Mesquita, L., McClenahan, D., Thornton, J., Carriere, J. & Wong, B. 2017: Drake Landing Solar Community: 10 years of operation. *International Energy Agency Solar Heating & Cooling Programme's International Conference on Solar Heating and Cooling for Buildings and Industry, International Solar Energy Society Solar World Conference Proceedings (2017), 29. October–2 November 2017, Abu Dhabi, United Arab Emirates*. https://doi.org/10.18086/swc.2017.06.09.

NVE. 2021: Åknes. https://www.nve.no/flaum-og-skred/fjellskredovervaking/kontinuerlig-overvakede-fjellpartier/aknes/ (accessed 22. February 2021).

Ramstad, R.K. 2004: *Ground source energy in crystalline bedrock - increased energy extraction by using hydraulic fracturing in boreholes*. PhD thesis, Norwegian University of Science and Technology, 185 pp.

Read, T., Bour, O., Bense, V., Le Borgne, T., Goderniaux, P., Klepikova, M., Hochreutener, R., Lavenant, N. & Boschero, V. 2013: Characterizing groundwater flow and heat transport in fractured rock using fiber-optic distributed temperature sensing. *Geophysical Research Letters 40*, 2055–2059. https://doi.org/10.1002/grl.50397.

Sena, C. & Braathen, A. 2020: Åknes rock-slope failure hydrogeology. *Second progress report on the collaboration project between the Department of Geosciences of the University of Oslo (UiO) and the Norges vassdrags- og energidirektorat (NVE)*, 35 pp.

Slagstad, T., Midttømme, K., Ramstad, R.K. & Slagstad, D. 2008: Factors influencing shallow (<1000 m depth) temperatures and their significance for extraction of ground-source heat. *In* Slagstad, T. (ed.): *Geology for Society*, Geological Survey of Norway Special Publication 11, pp. 99–109.

van de Giesen, N., Steele-Dunn, S., Jansen, J., Hoes, O., Hausner, M., Tyler, S. & Selker, J. 2012: Double-ended calibration of fiber-optic raman spectra distributed temperature sensing data. *Sensors 12*, 5471–5485. https://doi.org/10.3390/s120505471.

Walpole, R.E., Myers, R.H., Myers, S.L. & Ye, K. 2007: *Probability & Statistics for Engineers & Scientists* (8th edition). Upper Saddle River, Pearson Prentice Hall, p. 121.

Table 1. Data for the boreholes considered in this study from Elvebakk & Pless (2018).

Borehole name	Depth	Diameter [mm]	Altitude [amsl]	Measurement period
KH-01-17	304	96	507	June-August 2018
KH-02-17	300	96	734	June-August 2018
KH-01-18	221	96	593	June-August 2019
KH-02-18	200	96	482	June-August 2019

Table 2. Temperatures and vertical groundwater flow values used in the estimation of fracture groundwater flow: Temperature is abbreviated "temp." Minimum is abbreviated "min." and maximum is abbreviated "max." The second lowest temperature is denoted "2nd min temp."

Borehole	**Approximate depth [m]**	**Min. temp. (2nd min temp) [°C]**	**Max. temp. [°C]**	**Vertical downwards velocity from Acuña et al. (2018, 2020) [m/min]**
KH-01-17	78	3.0 (3.5)		0.16
	87	3.1 (3.6)		0.10
	99	3.2 (3.6)		0.10
KH-02-17	123		3.5	0.47
	267	2.5 (3.7)		0.67
	275	2.5 (3.6)		0.67
KH-01-18	75		5.1	-0.24
	133	5.1		-0.24
	198	5.3		-0.24
KH-02-18	90		5.6	-0.16
	125	5.3		-0.16
	138		6.2	0.00

Table 3. Estimated groundwater flow and their standard deviations for sections without visible fractures in boreholes KH-01-17 and KH-02-17. As the vertical flow for the section at 250-254 m depth in KH-02-17 is uncertain, two results with two different values for vertical flow are presented.

KH-01-17				KH-02-17			
Depth of section considered [m]	Asssumed vertical velocity [m/min]	Mean estimated flow rate [l/h]	Standard deviation [l/h]	Depth of section considered [m]	Asssumed vertical velocity [m/min]	Mean estimated flow rate [l/h]	Standard deviation [l/h]
60-63	0.16	-0.8	2.5	250-254	0.47	-1.1	0.35
105-110	0.16	-3	2.7	250-254	0.67	-1.5	0.5
200-204	0.16	-1.3	2.6	230-234	0.67	-2.6	0.39

*Table 4. Comparison of where active fractures were found in this study vs. two previous studies in the two borehole KH-01-17 and KH-02-17 at Åkneset, Norway: Depth values are approximate. *Changes in P- and S-waves found at the same depth. **Change in resistivity found at the same depth. *** No change in flowmeter value found at this depth, but consistent disturbance in flowmeter measurements both up and down.*

Active fractures found in this study		**Elvebakk & Pless (2018)**		**Acuna et al. (2018)**
Borehole	and depth [m]	Flowmeter	Temperature gradient	Heat tracer tests
KH-01-17	78		70-80	54-79
	87		90-110	
	99-100	99-100	90-110	99-104
KH-02-17	123	123		115-125
	267	Not drilled to these depths when test was performed		
	275		270-275	275
KH-01-18	75	66 and 86	75, *, **	
	133		132, *	
	198	178	196	
KH-02-18	125	130***	123	130

Figure 1. Maps of Åkneset from Kartverket (2021). Left: Åkneset, Norway labelled; Right: Overview of the boreholes at Åkneset considered in this study: boreholes are marked by red dots and their names are given in yellow. A blue dot shows the location of Åknes meterological station (c. 900 amsl). North is shown by the yellow arrow. Instevatnet (a lake) is also show in the upper left corner.

Figure 2. A control volume for estimation of groundwater groundwater flow in fractures/fracture zones ($\dot{m}_{in}$): the figure shows a cross-section of the borehole seen from the side, together with different energy groundwater flows in and out of the control volume. The orange arrows represent conductive heat, whereas the blue arrows represents advective heat. Note that groundwater flow into and out of the fracture(s) (i.e., $\dot{m}_{in}$ and $\dot{m}_{out}$) may differ, and that groundwater flowing out is assumed to have the average control volume temperature so that these terms become 0.

Figure 3. Sketch summarising the results for vertical groundwater flow (modified after Acuña et al. (2020), fig. 9). The borehole names and depths are written above and below each borehole, respectively. The groundwater levels are indicated by blue lines. Depths where water enters through fractures are given by green text and arrows, and depths where groundwater leaves the borehole through fractures are given by red text and arrows. The velocity of the vertical groundwater movement is written with larger, black letters.

Figure 4. Temperature profiles in the four boreholes at various times during the measurement periods: Upper left: KH-01-17; Upper right: KH-02-17; Lower left: KH-01-18 and Lower right: KH-02-18. The groundwater table (GWT) and identified fractures are marked by stippled lines. For all boreholes except KH-01-17, the groundwater table causes a visible shift in temperature and/or temperature gradient.

Figure 5. Estimated groundwater flow into the fracture at 125 m depth in KH-02-18

Figure 6. Correlation between moving daily averages of groundwater flow estimation at 78, 87 and 99 m depth in KH-01-17 and precipitation: The precipitation data are adjusted by 3.8–3.9 days, giving correlation factors of 0.69, 0.60 and 0.62. "Minimum inflow" is calculated based on that T_{in} in equation 5 equals the lowest measured temperature in the control volume, whereas "Minimum inflow" applies the second lowest measured temperature.*

Figure 7. Correlation between moving, average (daily) groundwater flow estimation at 123, 267 and 275 m depth in KH-02-17 and daily precipitation: the precipitation data are adjusted by 1.0, 1.1 and 0.9 days, which gives a correlation factor with precipitation of 0.17, 0.16 and 0.17 for the fractures in decreasing order.

Figure 8. Estimated groundwater flow in KH-01-18 (moving daily averages) and their correlation with precipitation (moving daily averages): No clear trend was found; the highest correlation factor was 0.11.

Figure 9. The left-hand side of the figure shows the estimated groundwater flows in KH-01-18 (moving daily averages) and their correlation with ambient temperature (moving daily averages): The highest correlation factor found was 0.68, when

temperature data were moved 9.0 days forward in time. The right side of the figure shows the estimated groundwater flow in KH-02-18 (moving daily averages) and its correlation with ambient temperature): The highest correlation factor found was 0.84, when temperature data were moved 1.4 days forward in time.

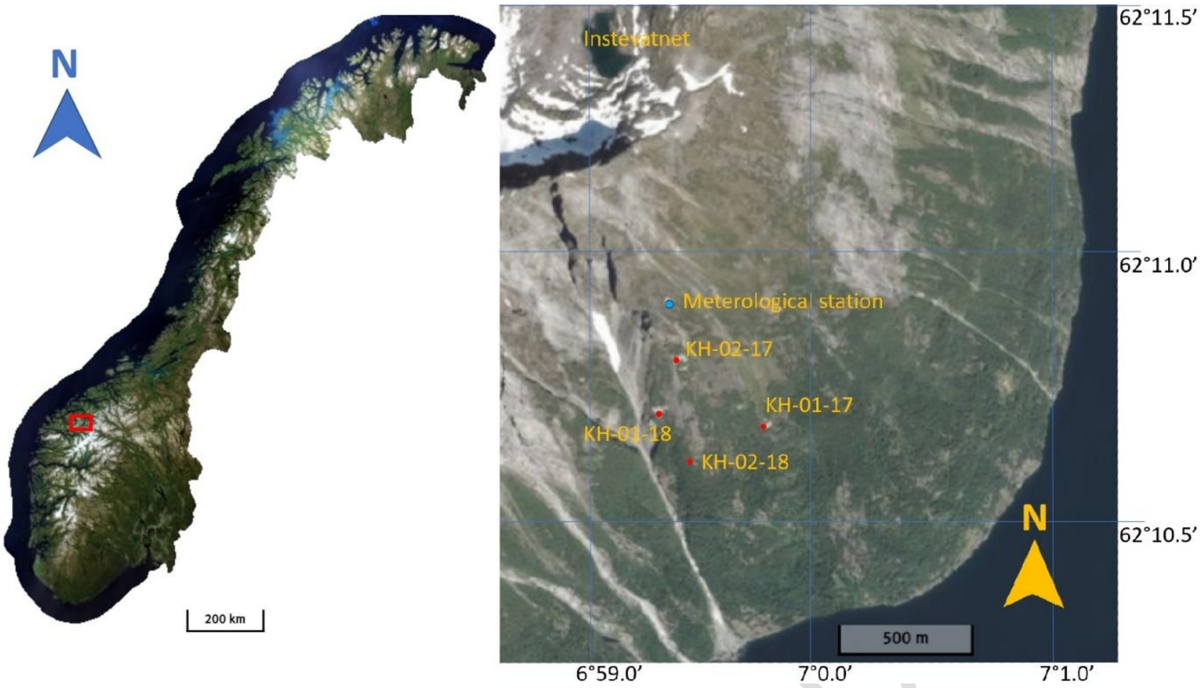

Figure 1. Maps of Åkneset from Kartverket (2021). Left: Åkneset, Norway labelled; Right: Overview of the boreholes at Åkneset considered in this study: boreholes are marked by red dots and their names are given in yellow. A blue dot shows the location of Åknes meterological station (c. 900 amsl). North is shown by the yellow arrow. Instevatnet (a lake) is also shown in the upper left corner.

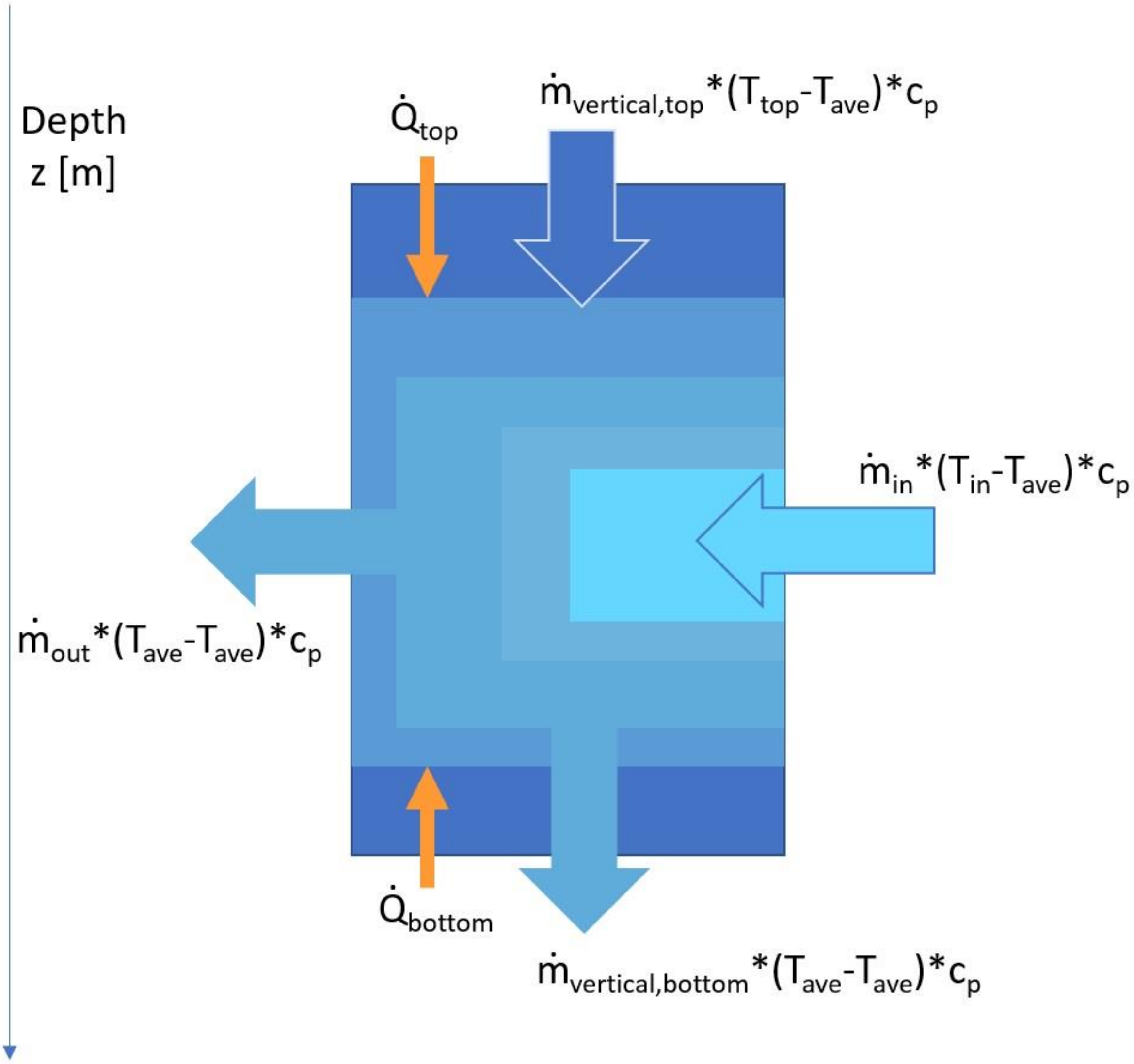

Figure 2. Control volume for estimation of groundwater groundwater flow in fractures/fracture zones ($\dot{m}_{in}$): the figure shows a cross-section of the borehole seen from the side, together with different energy groundwater flows in and out of the control volume. The orange arrows represent conductive heat, whereas the blue arrows represents advective heat. Notice that groundwater flow into and out of the fracture(s) (i.e., $\dot{m}_{in}$ and $\dot{m}_{out}$) may differ, and that groundwater flowing out is assumed to have the average control volume temperature so that these terms become 0.

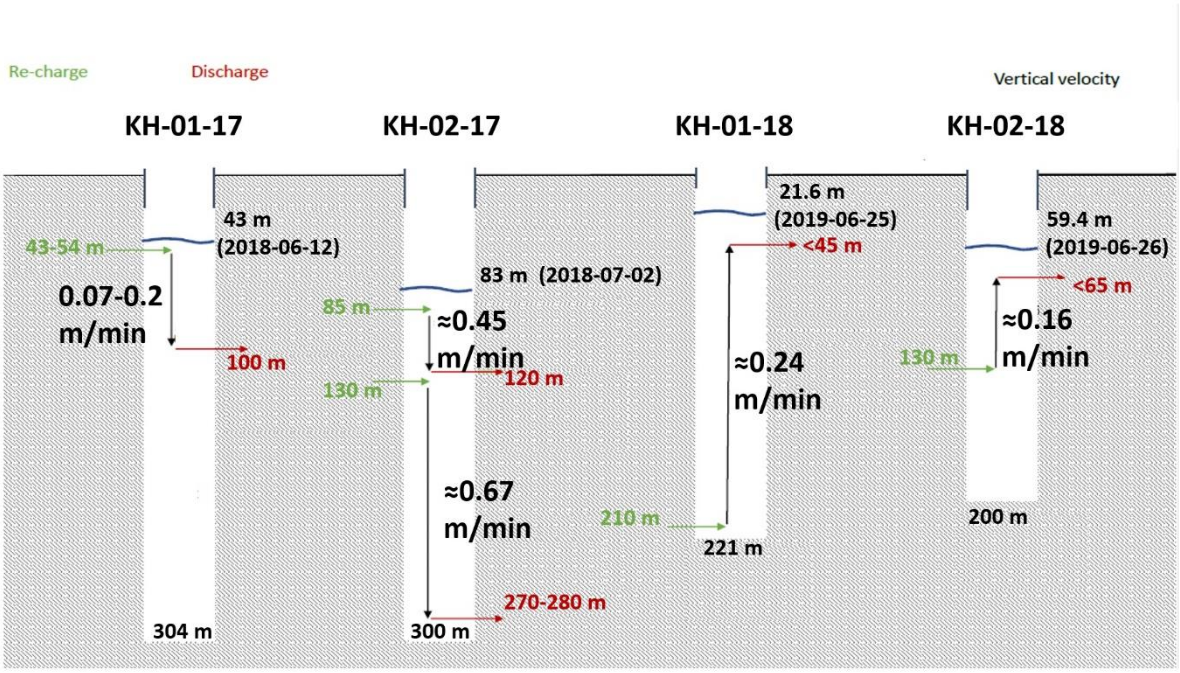

Figure 3. Sketch summarising the results for vertical groundwater flow (modified after Acuña et al. (2020), fig. 9). The borehole names and depths are written above and below each borehole, respectively. The groundwater levels are indicated by blue lines. Depths where water enters through fractures are given by green text and arrows, and depths where groundwater leaves the borehole through fractures are given by red text and arrows. The velocity of the vertical groundwater movement is written with larger, black letters.

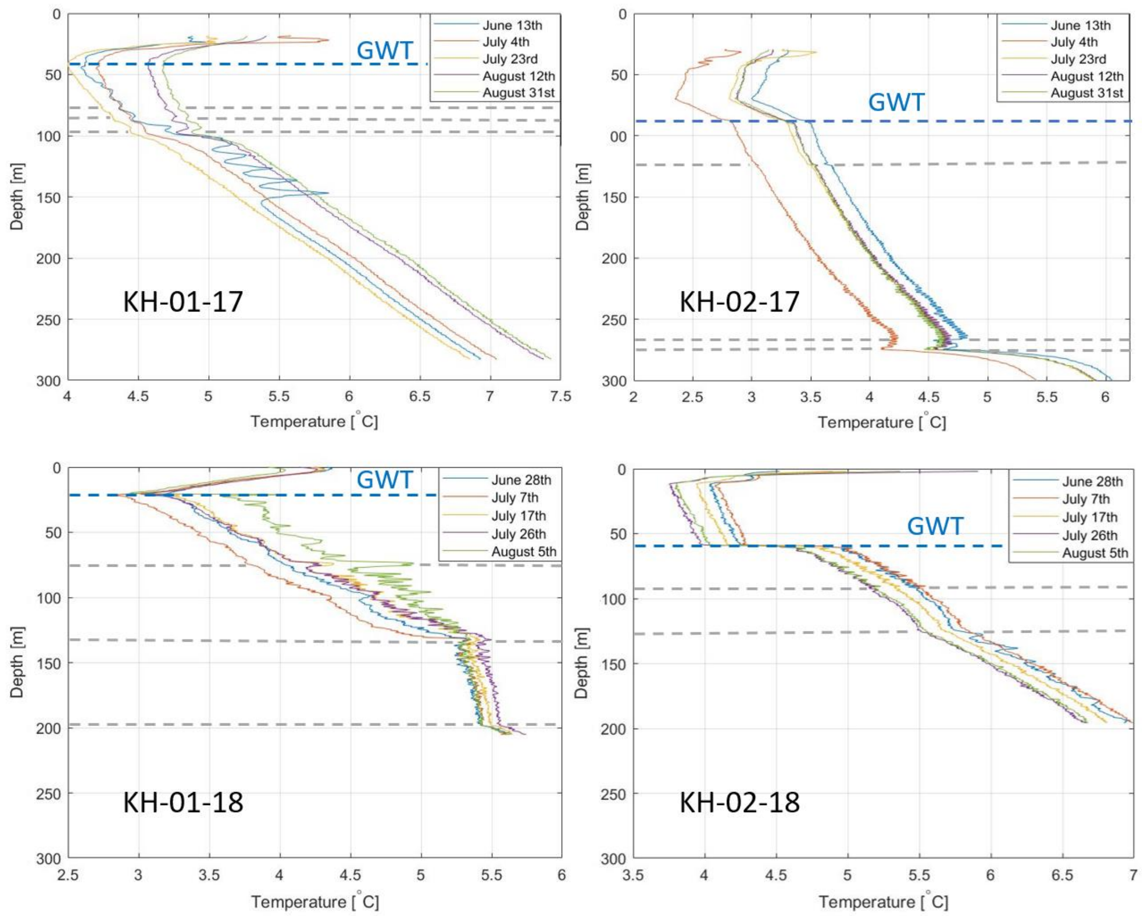

Figure 4. Temperature profiles in the four boreholes at various times during the measurement periods: Upper left: KH-01-17; Upper right: KH-02-17; Lower left: KH-01-18 and Lower right: KH-02-18. The groundwater table (GWT) and identified fractures are marked by stippled lines. For all boreholes except KH-01-17, the groundwater table causes a visible shift in temperature and/or temperature gradient.

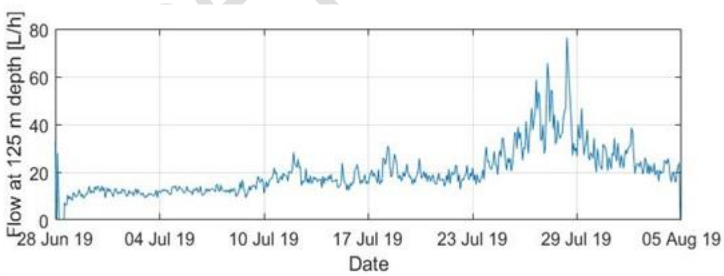

Figure 5. Estimated groundwater flow into the fracture at 125 m depth in KH-02-18

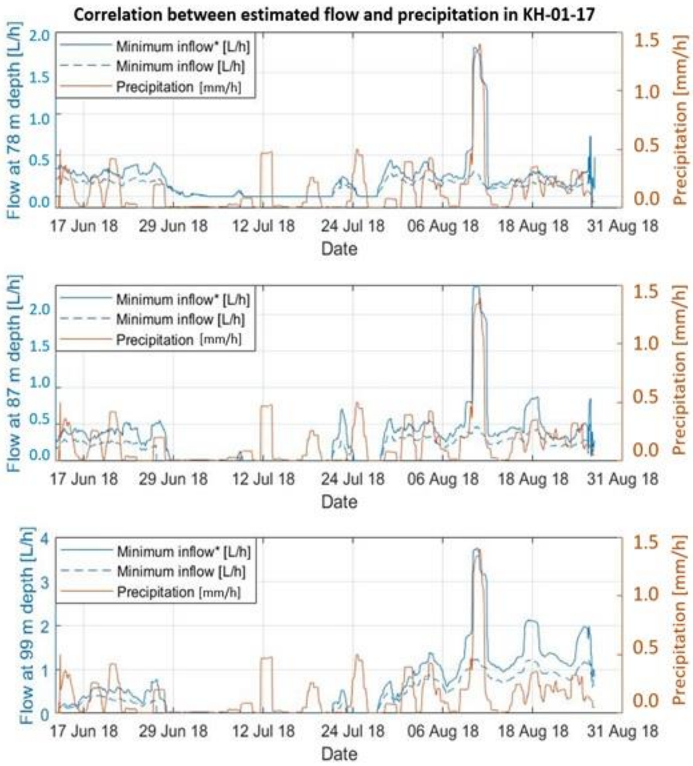

Figure 6. Correlation between moving daily averages of groundwater flow estimation at 78, 87 and 99 m depth in KH-01-17 and precipitation: The precipitation data are adjusted by 3.8–3.9 days, giving correlation factors of 0.69, 0.60 and 0.62. "Minimum inflow" is calculated based on that T_{in} in equation 5 equals the lowest measured temperature in the control volume, whereas "Minimum inflow" applies the second lowest measured temperature.*

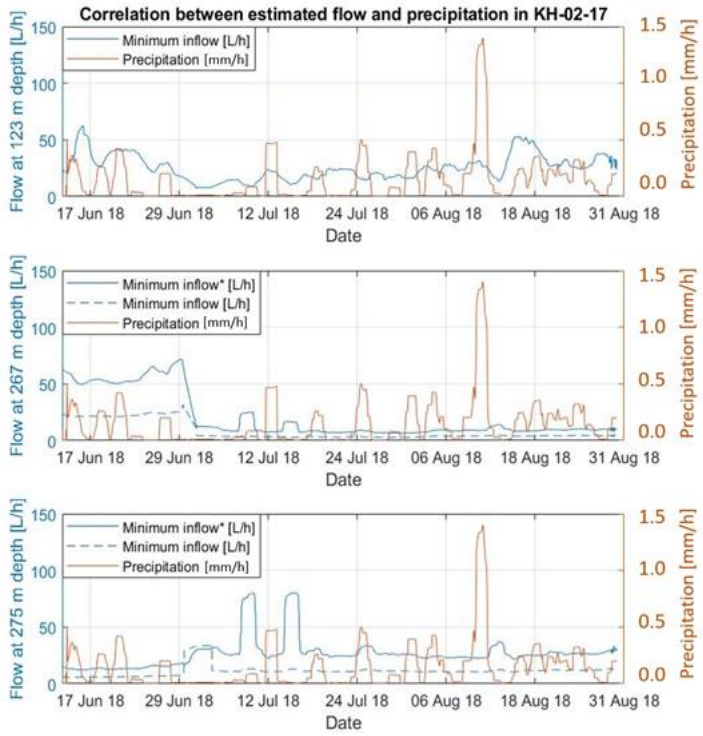

Figure 7. Correlation between moving, average (daily) groundwater flow estimation at 123, 267 and 275 m depth in KH-02-17 and daily precipitation: the precipitation data are adjusted by 1.0, 1.1 and 0.9 days, which gives a correlation factor with precipitation of 0.17, 0.16 and 0.17 for the fractures in decreasing order.

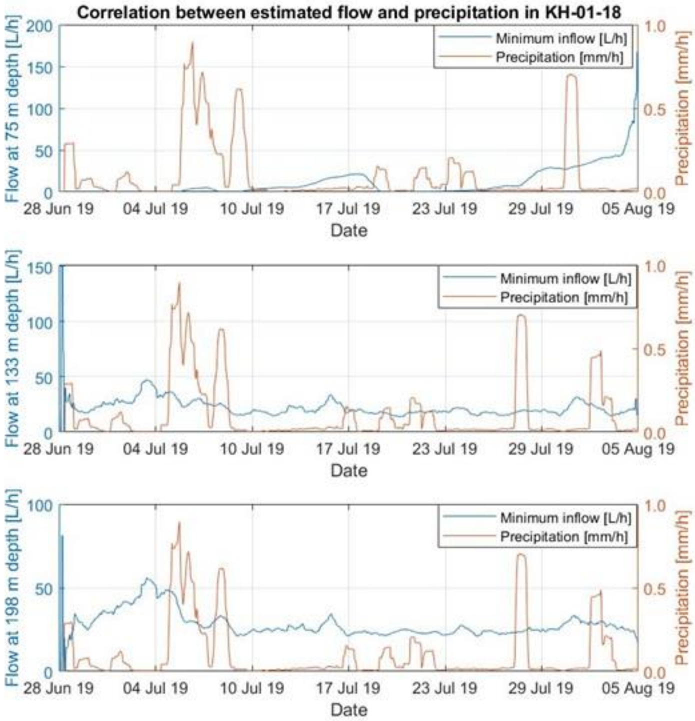

Figure 8. Estimated groundwater flow in KH-01-18 (moving daily averages) and their correlation with precipitation (moving daily averages): No clear trend was found; the highest correlation factor was 0.11.

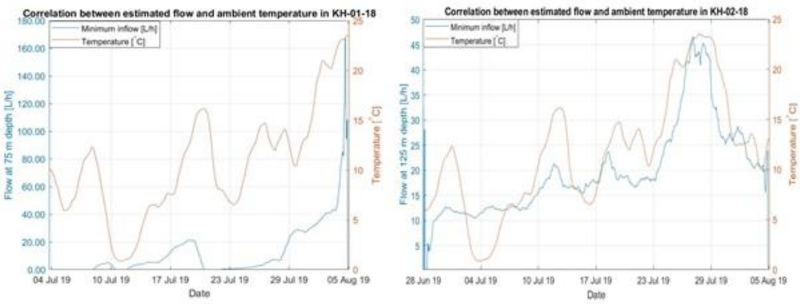

Figure 9. The left-hand side of the figure shows the estimated groundwater flow in KH-01-18 (moving daily averages) and their correlation with ambient temperature (moving daily averages): The highest correlation factor found was 0.68, when temperature data were moved 9.0 days forward in time. The right side of the figure shows the estimated groundwater flow in KH-02-18 (moving daily averages) and its correlation with ambient temperature): The highest correlation factor found was 0.84, when temperature data were moved 1.4 days forward in time.